# STIM1 controls calcineurin/Akt/mTOR/NFATC2-mediated osteoclastogenesis induced by RANKL/M-CSF

YANJIAO HUANG[1], QIANG LI[2], ZUNYONG FENG[3] and LANRONG ZHENG[1]

Departments of [1]Pathological Anatomy, [2]Anatomy and [3]Forensic Medicine, Wannan Medical College, Wuhu, Anhui 241002, P.R. China

Received October 15, 2018; Accepted June 20, 2019

DOI: 10.3892/etm.2020.8774

**Abstract.** Store-operated $Ca^{2+}$ entry (SOCE) is the stable calcium channel influx in most cells. It consists of the cytoplasmic ion channel ORAI and endoplasmic reticulum receptor stromal interaction molecule 1 (STIM1). Abolition of SOCE function due to ORAI1 and STIM1 gene defects may cause non-perspiration, ectoderm dysplasia and skeletal malformations with severe combined immunodeficiency (CID). Calcineurin/mammalian target of rapamycin (mTOR)/nuclear factor of activated T cells 2 (NFATC2) is an important signalling cascade for osteoclast development. Calcineurin is activated by $Ca^{2+}$ via SOCE during osteoclastogenesis, which is induced by receptor activator of NF-κB ligand (RANKL) and macrophage colony-stimulating factor (M-CSF). However, the underlying mechanism has remained to be fully elucidated, which was therefore the aim of the present study. In the current study, flow cytometry was used to examine the effect of a number of STIM1 mutations on proliferation, differentiation, and expression of osteolysis-associated proteins in Bone marrow-derived mononuclear macrophages (BMDM). The calcineurin/AKT/mTOR/NFATC2 signaling cascade activation were also assessed. BMDMs were obtained from three patients with STIM1 mutations (p.E136X, p.R429C and p.R304W). These mutations, which exhibited abolished (p.E136X, p.R429C) or constitutively activated (p.R304W) SOCE, failed to respond to RANKL/M-CSF-mediated induction of normal osteoclastogenesis. In addition, activation of the calcineurin/Akt/mTOR/NFATC2 signalling cascade induced by RANKL/M-CSF was abnormal in the BMDMs with STIM1 mutants compared with that in BMDMs from healthy subjects. In addition, overexpression of wild-type STIM1 restored SOCE in p.R429C- and p.E136X-mutant BMDMs, but not in p.R304W-mutant BMDMs. Of note, calcineurin, cyclosporin A, mTOR inhibitor rapamycin and NFATC2-specific small interfering RNA restored the function of SOCE in p.R304W-mutant BMDMs. The present study suggests a role for SOCE in calcineurin/Akt/mTOR/NFATC2-mediated osteoclast proliferation, differentiation and function.

## Introduction

Bone homeostasis is maintained by the balance between bone resorption by osteoclasts and bone formation by osteoblasts. Osteoclasts are derived from the bone marrow-derived mononuclear-macrophage (BMDM) cell lineage and osteoblasts are derived from mesenchymal cells (1-3). Osteoclasts are the only type of bone-resorbing cell that are essential for bone development and remodelling, and their lack leads to osteopetrosis, which is a disease manifested by an increase in the non-proliferating bone mass (4). Conversely, increased numbers and activity of osteoclasts under certain pathological conditions lead to accelerated bone resorption and may lead to osteoporosis and osteolytic diseases (5,6). To better understand the mechanism of osteoclast-based diseases and develop relevant therapeutic methods, the molecular basis of osteoclast differentiation and function, and the regulatory mechanisms of osteoclast signalling must be elucidated.

Numerous studies have confirmed that receptor activator of NF-κB ligand (RANKL) is an important extracellular regulatory molecule for osteoclast development that stimulates osteoclast formation (5,7). Binding of RANKL to its receptor leads to recruitment of tumour necrosis factor receptor-associated factor 6 and activation of NF-κB/mitogen-activated protein kinase (MAPK) signalling, which is the most direct pathway for osteoclast development (8). In addition, calcineurin/mammalian target of rapamycin (mTOR)/nuclear factor of activated T cells 2 (NFATC2) signalling has an important role in RANKL-induced osteoclast development (9-11).

*Correspondence to:* Dr Lanrong Zheng, Department of Pathological Anatomy, Wannan Medical College, 22 Wen Chang West Road, Wuhu, Anhui 241002, P.R. China
E-mail: zhenglanrong@foxmail.com

*Abbreviations:* SOCE, store-operated $Ca^{2+}$ entry; RANKL, receptor activator of NF-κB ligand; M-CSF, macrophage colony-stimulating factor; BMDMs, bone marrow-derived mononuclear macrophages; CsA, cyclosporin A; Rap, rapamycin; CID, combined immunodeficiency; ER, endoplasmic reticulum; CRAC, $Ca^{2+}$ release-activated $Ca^{2+}$ channel; mTOR, mammalian target of rapamycin; SNP, single nucleotide polymorphism; CaN, calcineurin; TG, thapsigargin

*Key words:* stromal interaction molecule 1, store-operated $Ca^{2+}$ entry, osteoclastogenesis, calcineurin, mTOR, nuclear factor of activated T-cells 2

Calcineurin and mTOR are important negative regulators during bone development, and their respective clinical target drugs cyclosporin A (CsA) and rapamycin cause severe bone metabolic disease (12-14). NFATC2 is a direct regulatory transcription factor for osteoclast development that regulates osteoclastogenesis, as well as the expression of osteolysis-associated molecules, including matrix metallopeptidase (MMP)-9 and cathepsin K (5,10,15). Activation of calcineurin/mTOR/NFATC2 is dependent on the intracellular $Ca^{2+}$ levels. The RANKL-induced calcium influx-activated calcineurin-dependent NFATC2 pathway has been reported to have an important role in osteoclast differentiation (16); these authors observed a continuous rather than a transient calcium influx, which was critical for the continued activation of NFATC2. However, how RANKL leads to activation and nuclear translocation of NFATC2 via activation of the calcium influx has remained elusive. The involvement in RANKL-induced osteoblast differentiation has been reported for calcium influx mediated by transmembrane protein 64 by Kim *et al* (17), the Transient receptor potential cation channel subfamily V member 4 channel by Masuyama *et al* (18) and the store-operated $Ca^{2+}$ entry (SOCE) membrane calcium channel ORAI1 by Hwang and Putney (19); importantly, these calcium influxes regulate osteoclast development through sustained activation of NFATC2 and nuclear translocation. However, few studies have investigated RANKL-induced osteoclast differentiation via the endoplasmic reticulum (ER) sensor stromal interaction molecule 1 (STIM1) of SOCE.

Combined immunodeficiencies (CID) are genetic defects that result in defective T cell function with or without intrinsic B cell abnormalities. The CID caused by the *STIM1* gene mutation is called the Stormorken Syndrome. In the present study, three STIM1 mutations were identified in patients with Stormorken Syndrome; (the p.E136X recessive mutation, p.R429C dominant mutation and p.R304W recessive mutation). The three patients had different degrees of skeletal sclerosis (p.E136X and p.R429C) and bone loss (p.R304W) disease. Osteoclast precursor cells, which are BMDMs, were obtained from these patients and a healthy individual, and subjected to *in vitro* experiments. The osteoclast differentiation phenotype induced by RANKL/macrophage colony-stimulating factor (M-CSF) was observed and the signalling pathways involved in calcium influx via SOCE were investigated.

## Materials and methods

*Subjects*. BMDM samples were obtained from three male CID patients (age, Patient 1, 4 years; Patient 2, 4 years; and Patient 3, 7 years) and one healthy male subject (age, 17 years. For the healthy subject, bone marrow sample was obtained due to suspected aplastic anemia, where part of the BMDM are used for *in vitro* culture. The patient' final diagnosis was negative for aplastic anemia. The experiments involving human subjects were based on the Declaration of Helsinki and the European Declaration of Human Rights, and informed consent was obtained from the parents of the patients and the healthy donor. The study was approved by the Ethical Review Committee of Yanjishan Hospital of Wannan Medical College (Wuhu, China; no. 201627). Bone mineral density (BMD) of the L1-4 lumbar vertebrae and left hip (femoral neck, total hip joint) were measured by Hologic dual-energy X-ray absorptiometry (Hologic). The BMD was provided as the bone mineral content per unit area in $mg/cm^2$. As shown in Table II, the Z value is provided by Hologic, Inc. and is compared with the BMD value of the corresponding age average in the Asian Children's Database (20,21). Healthy was defined as 1>Z value >-1; Mild low bone density as -1<Z; Low bone density as -1.5<Z value<-1, Moderate loss for bone density as -2<Z value <-1.5; and Severe loss for bone density as Z<-2.

*Genomic sequencing*. Genomic DNA was isolated from skin fibroblasts of CID patients and the healthy control using DNAzol Reagent (Thermo Fisher Scientific, Inc.) according to manufacturer's protocol. High-fidelity KOD DNA polymerase (Biosciences) was used to PCR-amplify the STIM1 exon sequence. The primer sequences were as follows: Forward, 5'-CTTAACTGTTCG GGGACACA-3' and reverse, 5'-ACAGCGGAAGAGTGACAC TG-3'. The amplicons were purified with the QIAquick Gel Extraction kit (Qiagen GmbH) and directly sent for sequencing (Genewiz, Inc.). If a mutation was detected, the PCR and sequencing reactions were repeated a further three times using at least two separate genomic DNA preparations. Sequence alignments were performed using T-Coffee software (Swiss Institute of Bioinformatics) (22); DNA sequencing traces were presented using PeakTrace Basecaller software (version 6.46; Nucleics Pty., Ltd.). Single-nucleotide polymorphism (SNP) searches were performed in the dbSNP database (www.ncbi.nlm.nih.gov/SNP) of the National Council for Biotechnology Information.

*Acquisition of BMDMs*. A total of 2 ml bone marrow samples was collected in a sterile polyacrylamide centrifuge tube using a non-invasive Sprotte spinal needle (Pajunk) and centrifuged to separate the cells and debris (2,000 x g, 4˚C, 5 min). The supernatant was discarded and the pellet was re-suspended in red blood cell lysis buffer, followed by incubation at 4˚C for 10 min. The cells were centrifuged, re-suspended and counted, and the concentration was adjusted to $2x10^6$ cells/ml. The cells were cultured in 37˚C in a humidified atmosphere with 5% $CO_2$, and grown in complete Dulbecco's modified Eagle's medium (DMEM, Gibco; Thermo Fisher Scientific, Inc.) containing 10% fetal bovine serum (FBS, Gibco; Thermo Fisher Scientific, Inc.) and 5 ng/ml M-CSF to ensure survival of the BMDMs. The medium was replaced every 2-3 days and mature BMDMs were harvested after 7 days. Mature BMDMs were stored in complete DMEM containing 1% DMSO and 10% FBS at -20˚C for use in subsequent experiments. pGMLV-SV40T lentivirus (Genomeditech Co. Ltd.) was used for immortalization of the BMDM cells. The immortalized cell line was generated by transfecting primary BMDM cells with a vector expressing the oncogene pSV40Tag for 72 h, in accordance with a protocol established previously (23). Its characteristics are maintained in the media aforementioned for >30 generations where no cell differentiation or lack of proliferation were observed.

*Plasmids and antibodies*. Plasmid vectors encoding wild type STIM1 (MIGR-STIM1-IRES-RFP, ca.STIM1 thereafter), and NFATC2 small interfering (si)RNA were constructed by Shanghai GenePharma Co., Ltd. The species reactivity, conjugation, manufacturer, product catalog numbers and dilutions of all antibodies used are shown in Table I.

Table I. Information of all antibodies used in the present study.

| Name | Host | Species reactivity | Conjugation | Supplier | Cat. no. | Dilution used |
|---|---|---|---|---|---|---|
| STIM1 | Rabbit | Human | Unconjugated | Cell Signaling Technology, Inc. | 5668 | 1:20 (FC) |
| CD11b | Mouse | Human | Unconjugated | Abcam | Ab34216 | 1:50 (FC) |
| TRAP | Rabbit | Human | Unconjugated | Abcam | ab2391 | 1:50 (FC) |
| Ki67 | Rabbit | Human | Alexa Fluor 488 | Cell Signaling Technology, Inc. | 11882 | 1:50 (FC) |
| p-mTOR | Rabbit | Human | Unconjugated | Cell Signaling Technology, Inc. | 5536 | 1:20 (FC) |
| p-AKT (T308) | Rabbit | Human | Unconjugated | Cell Signaling Technology, Inc. | 13038 | 1:20 (FC) |
| p-AKT (S473) | Rabbit | Human | Unconjugated | Cell Signaling Technology, Inc. | 4060 | 1:20 (FC) |
| p-S6 (S235/236) | Rabbit | Human | Unconjugated | Cell Signaling Technology, Inc. | 4858 | 1:20 (FC) |
| p-NFATC2 (Ser54) | Rabbit | Human | Unconjugated | eBioscience; Thermo Fisher Scientific, Inc. | 44-944G | 1:20 (FC) |
| NFATC2 | Mouse | Human | Unconjugated | R&D Systems | MAB6499 | 1:20 (FC) |
| MMP9 | Rabbit | Human | Unconjugated | Cell Signaling Technology, Inc. | 13667 | 1:50 (FC) |
| Cathepsin K | Rabbit | Human | Unconjugated | eBioscience; Thermo Fisher Scientific, Inc. | PA5-14270 | 1:50 (FC) |
| Secondary antibody | Goat | Rabbit | Alexa Fluor 647 | Thermo Fisher Scientific, Inc. | A32733 | 1:100 (FC) |
| Secondary antibody | Goat | Mouse | Alexa Fluor 488 | Thermo Fisher Scientific, Inc. | A28175 | 1:100 (FC) |
| (FcgR)II/FcgRIII | Mouse | Human | Unconjugated | eBioscience; Thermo Fisher Scientific, Inc. | MFCR00-4 | 1:100 (FC) |

STIM1, stromal interaction molecule 1; CD11b, integrin alpha M; TRAP, triiodothyronine receptor auxiliary protein; mTOR, mechanistic target of rapamycin kinase; S6, protein S6; NFATC2, nuclear factor of activated T cells 2; MMP9, matrix metallopeptidase 9; (FcgR)II/FcgRIII, Fc fragment of IgG receptor II/III; FC, Flow cytometry.

Table II. Bone mineral density (mg/cm$^2$) and Z value of stromal interaction molecule 1 mutation patients and a healthy subject.

| | Femoral neck | | Wards triangle | | Hip joint | | Lumbar spine L1-L4 | |
|---|---|---|---|---|---|---|---|---|
| STIM1 status | BMD | Z-value | BMD | Z-value | BMD | Z-value | BMD | Z-value |
| WT | 911.3 | 0.12 | 751.2 | 0.32 | 1019.3 | 0.41 | 1124.7 | 0.57 |
| p.E136X | 1125.7 | 1.51 | 895.8 | 1.35 | 1158.4 | 1.6 | 1354.6 | 1.52 |
| p.R429C | 1185.4 | 1.59 | 862.3 | 1.3 | 1162.3 | 1.61 | 1248.6 | 1.4 |
| p.R304W | 703.6 | -1.17 | 451.9 | -1.84 | 812.3 | -1.23 | 815.5 | -1.45 |

Healthy (1>Z value >-1); Mild low bone density (-1<Z); Low bone density (-1.5<Z value<-1), Moderate loss for bone density (-2<Z value <-1.5), Severe loss for bone density (Z<-2). WT, wild-type; STIM1, stromal interaction molecule 1.

*Flow cytometry*. Since the three naturally-mutant strains are rare (24) and the number of cells obtained is insufficient to detect protein expression using western blot analysis, the expression of all proteins was detected by flow cytometry. BMDMs were treated with rapamycin (0.1 nM; AdooQ Bioscience) and CsA (7 nM; AdooQ) or lentiviral concentrate. After 3 days of stimulation with recombinant human M-CSF (20 ng/ml; Kexin Biomedical Technology), the BMDMs were induced using 100 ng/ml RANKL (ACROBiosystems) for 3 days. The cells were treated with intracellular immobilization buffer (Thermo Fisher Scientific, Inc.) and blocked with an anti-Fc region of immunoglobulin receptor (FcgR) II/FcgRIII antibody for 2 h. The permeabilized cells were fixed by the slow addition of ice-cold 100% methanol to the pre-chilled cells under gentle vortexing, to a final concentration of 90% methanol. The cells were incubated with anti-STIM1, CD11b, TRAP, anti-Ki67, p-mTOR (S2448), phosphorylated (p)-AKT (T308), p-AKT (S473), p-S6 (S235/236), p-NFATC2, anti-MMP9 or anti-Cathepsin K primary antibodies overnight at 4˚C. A fluorescently labelled secondary antibody was coupled to the primary antibody for 2 h at room temperature in the dark. All flow cytometry experiments were also performed with homotyped non-specific negative control antibodies. The samples were analysed using the BD FACSCanto™ II flow cytometer (BD Biosciences).

*Carboxyfluorescein succinimidyl ester (CFSE) labelling of live cells*. BMDMs ($1x10^5$/ml) subjected to different treatments were loaded with 10 $\mu$M CFSE (eBioscience; Thermo Fisher Scientific, Inc.) according to the manufacturer's protocol. The cells were evaluated by flow cytometry using an excitation wavelength of 494 nm and emission wavelength of 521 nm.

*Lentiviral transfection*. The siRNA for NFATC2, scrambled siRNA, STIM1 overexpression plasmids and control plasmids were purchased from Genomeditech Co. Ltd. For each transfection reaction, 4 $\mu$g/ml SiRNA or 4 $\mu$g/ml plasmids and 10 $\mu$g/ml of the PPACK packaging plasmid (System Biosciences) were co-transfected into 293T cells (American Type Culture Collection) using Lipofectamine® 3000 (Thermo Fisher Scientific, Inc.) according to manufacturer's protocol. The 293T cells were cultured in DMEM supplemented with 10% FBS and 2 mM L-glutamine in 37˚C in a humidified atmosphere with 5% $CO_2$. After 2 days, the supernatant was collected and filtered by centrifugation in Amicon Ultra-15-centrifugal filter tubes according to the manufacturer's protocol. (Merck Millipore; Merck KGaA). The viral titres were determined by gradient dilution. The resulting concentrated lentiviral fluid was used for direct infection of BMDMs. The BMDM cell suspension was seeded into a 6-well plate and cultured overnight under the same conditions; the corresponding lentiviral solution (multiplicity of infection, 20) was added to the cells, followed by culture for 72 h. Subsequently, the cells were harvested, and the NFATC2-knockdown and STIM1-overexpressing cells were subjected to flow cytometric assays.

*Determination of intracellular $Ca^{2+}$ concentration*. A total of $5x10^3$ BMDMs were seeded onto poly-L-lysine-coated 96-well plates for attachment. The cells were first loaded with 1 mM Fura-2-AM (AAT Bioquest) and re-suspended using $Ca^{2+}$-free saline. Fluorescence intensity measurements were performed using an Epoch full wavelength microplate reader (Omega Bio-Tek, Inc.). After 250 sec, 30 nM thapsigargin (Abcam) was added to induce $Ca^{2+}$ release from the ER, and an equal volume of 40 mM $Ca^{2+}$ physiological saline solution was added at 500 sec to induce SOCE. Fura-2 fluorescence was excited at 340 and 380 nm, with their emission measured at 510 nm and plotted as the 340/380 nm ratio to represent the relative intracellular $Ca^{2+}$ levels.

*Detection of calcineurin activity*. After collection of the $5x10^4$ BMDMs treated with M-CSF/RANKL in the presence or absence of CsA, the cells were incubated with DMSO for 30 min and then stimulated with 10 nM caerulein for 15 min. The cells were lysed and the calcineurin activity was determined using the Calcineurin Cell Activity Assay kit (Abcam) according to the manufacturer's protocol.

*Detection of the cell proliferation activity*. A total of $5x10^3$ BMDMs were seeded into 96-well plates and treated with CsA, Rap, NFATC2 siRNA and ca.STIM1 or negative controls. The cells were then incubated with 10 $\mu$l Cell Counting Kit-8 stain (Dojindo Molecular Technologies, Inc.) for 2 h according to the manufacturer's protocol, and the absorbance at 450 nm was detected by a microplate reader (Omega Bio-Tek, Inc.).

*Statistical analysis*. The data were analysed using one-way analysis of variance and paired Student's t-test. The statistical analyses and graphical representation of the data were performed using GraphPad Prism 6.0 (GraphPad Inc.) and SPSS version 19.0 (IBM Corp.). $P<0.05$ was considered to indicate a statistically significant difference.

## Results

*Defects in STIM1 cause a disorder in SOCE in BMDMs*. Genomic DNA sequencing of patient 1 revealed a 380_381insA mutation resulting in insertion of an adenine between positions 380 and 381 in the exon 3 sequence of STIM1 (Fig. 1A). This mutation caused a change in 8 amino acids (RSIQLDRG) and led to a nonsense mutation and premature termination of the STIM1 translation codon (p.E136X; Fig. 1D). Patient 2 developed a C→T substitution mutation (c.1285C>T) at position 1,285 of exon 11 of STIM1 (Fig. 1B), which was a missense mutation that resulted in a single amino acid change in the STIM1 sequence (p.R429C; Fig. 1D). Patient 3 developed a C→T substitution mutation (c.910C>T) at position 910 of exon 6 of STIM1 (Fig. 1C), which resulted in a missense mutation in a single amino acid position in the STIM1 sequence (p.R304W; Fig. 1D). The p.E136X and p.R429C mutations resulted in loss of STIM1 expression, while p.R304W mutations had no effect on STIM1 expression (Fig. 1E). Studies have indicated that p.E136X and p.R429C mutations result in truncation of STIM1 during its expression and conformational changes, causing loss of function of SOCE (25,26), while p.R304W mutations cause conformational changes in STIM1 leading to constitutive activation of SOCE (27). The STIM1-wild-type ($STIM1^{wt}$) BMDMs produced transient $Ca^{2+}$ release from the ER in response to thapsigargin (TG), a Sarco ER calcium adenosine triphosphatase pump blocker, followed by an increase in the $Ca^{2+}$ concentration in the medium, leading to sustained extracellular $Ca^{2+}$ influx which is SOCE (Fig. 1F). This normal SOCE was abolished in BMDMs with $STIM1^{p.E136X}$ and $STIM1^{p.R429C}$ mutations, which responded to the TG-induced $Ca^{2+}$ release from the ER, but extracellular $Ca^{2+}$ did not enter the cell even after ER storage depletion (Fig. 1F). For BMDMs with $STIM1^{p.R304W}$ mutations, the intracellular $Ca^{2+}$ concentration varies with the extracellular $Ca^{2+}$, suggesting that their SOCE channel is continuously open (Fig. 1F). More importantly, three STIM1-mutant patients had a disorder of bone metabolism, indicating that the BMD of patients with p.R304W was too low, while the BMD of patients with p.E136X and p.R429C was too high (Table II). These results suggest that mutations in STIM1 affect the function of SOCE in BMDMs, which may be associated with bone metabolic disorders in patients carrying these mutations.

*STIM1 deficiency causes BMDM proliferation and differentiation disorders in response to RANKL/M-CSF*. RANKL/M-CSF treatment induced calcium influx in BMDM cells but did not alter STIM1 expression in BMDMs (Fig. 2A and B), suggestive of SOCE activation. STIM1 mutations cause disorder of RANKL/M-CSF-induced calcium influx in BMDMs, including elevated basic calcium levels in the $STIM1^{p.R304W}$ BMDMs, no sensitive calcium influx in $STIM1^{p.R429C}$ BMDMs and no response in $STIM1^{p.E136X}$ BMDMs (Fig. 2B). The

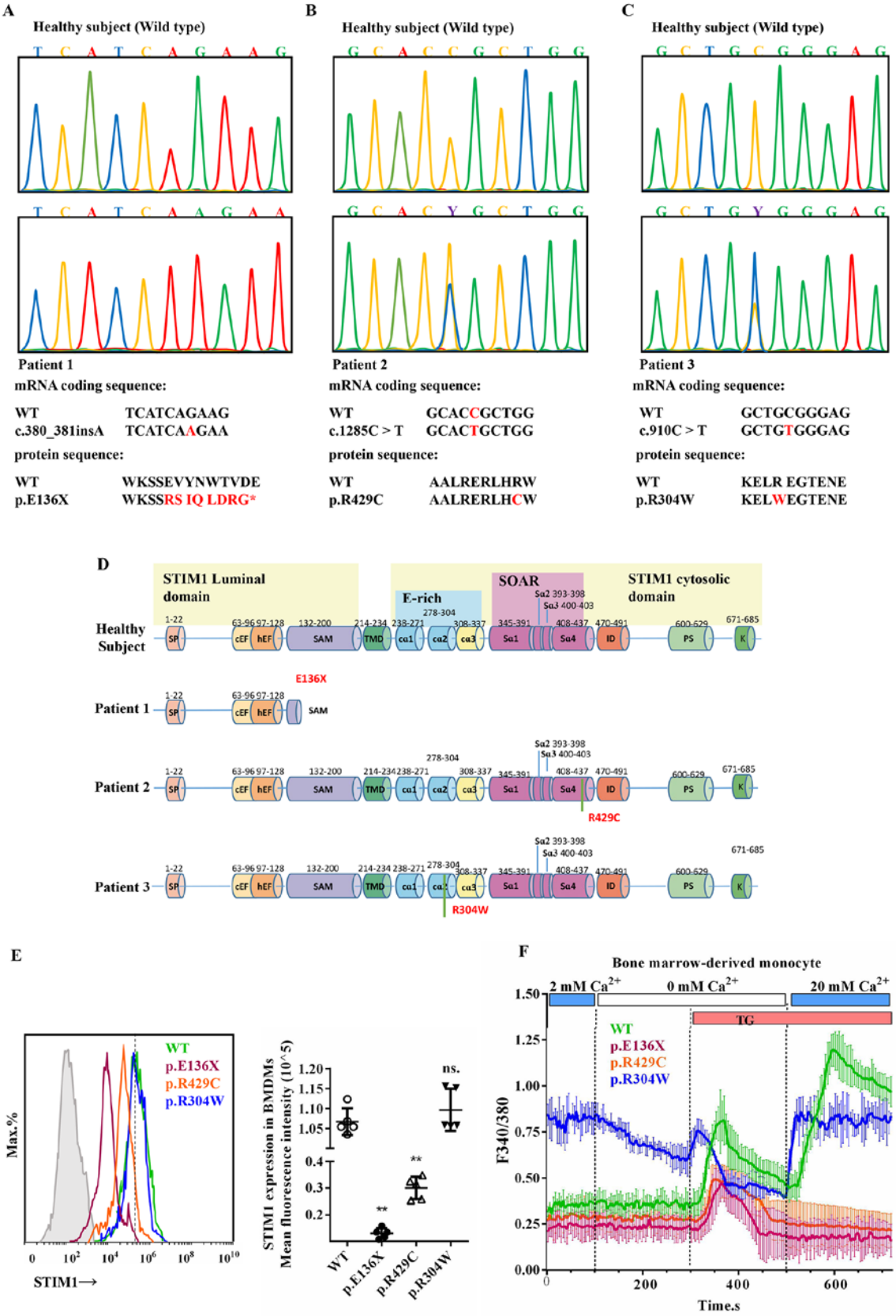


Figure 1. Missense or nonsense mutations in STIM1 cause disorder of the SOCE in BMDMs. (A-C) Sequence analysis of genomic STIM1 DNA obtained from (A) subject 1, (B) subject 2, (C) subject 3 and comparison with the corresponding sequence of the healthy subject. (D) Linear patterns of the normal and mutated STIM1 proteins. (E) STIM1 expression in BMDMs from patients with the mutations STIM1$^{p.E136X}$, STIM1$^{p.r429c}$ and STIM1$^{p.r304w}$, and the healthy subject. (F) The 340/380 nm ratio in Fura-2-loaded BMDMs from patients carrying the mutations STIM1$^{p.E136X}$, STIM1$^{p.r429c}$ and STIM1$^{p.r304w}$, and the healthy subject. TG was used to empty the intracellular $Ca^{2+}$ stores in the absence of extracellular $Ca^{2+}$ (0 mM $Ca^{2+}$) and SOCE was measured by addition of 20 mM extracellular $Ca^{2+}$. Values are expressed as the mean ± standard deviation (n=6). $^{**}$P<0.01 vs. WT BMDMs; ns, no significance vs. WT BMDMs. WT, wild-type; SOCE, store-operated $Ca^{2+}$ entry; STIM1, stromal interaction molecule 1; BMDMs, bone marrow-derived mononuclear macrophages; TG, thapsigargin. SOAR, STIM1-Orai1 activation region.

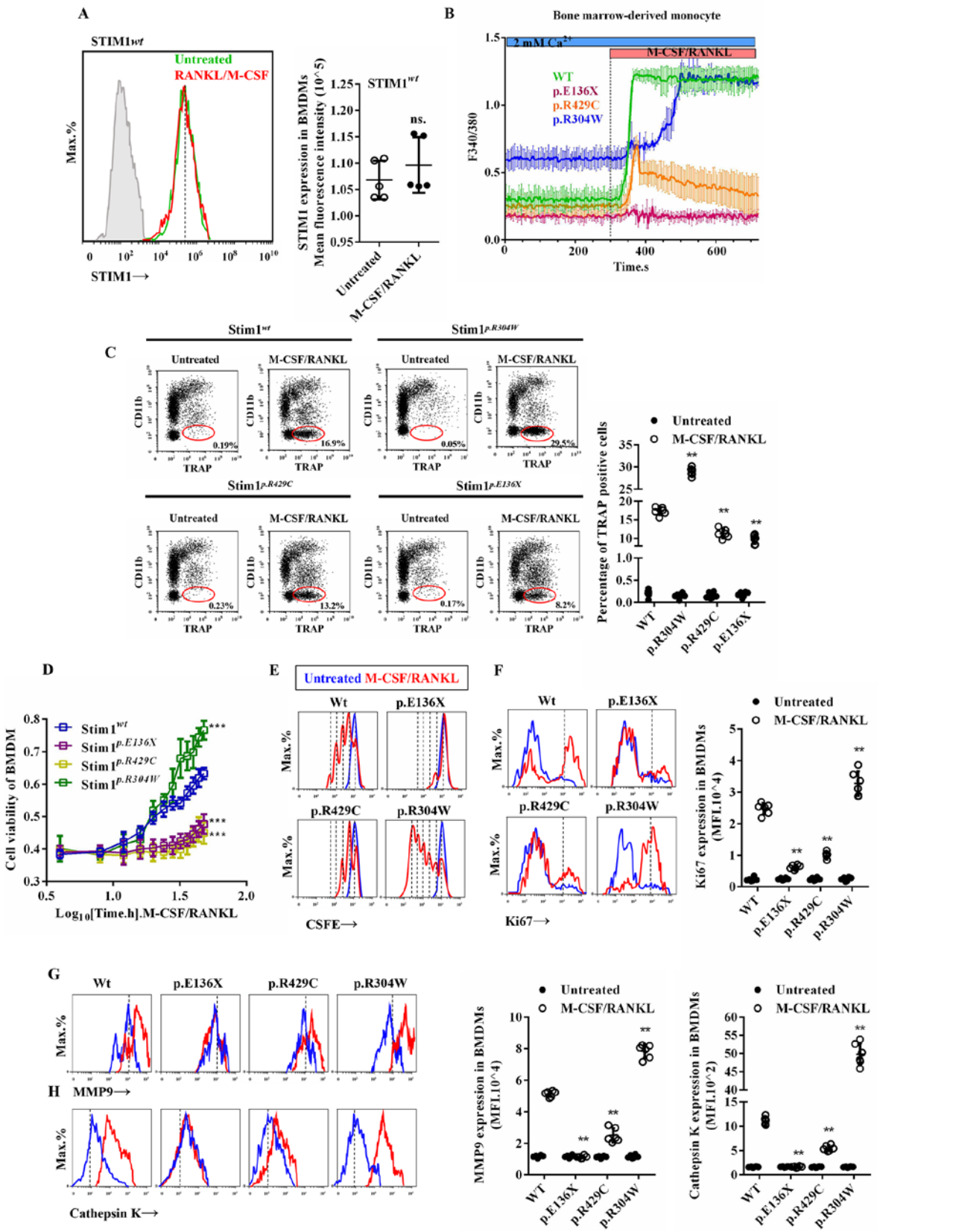


Figure 2. STIM1 deficiency affects BMDM proliferation and differentiation. (A) Expression of STIM1 in BMDMs of a healthy subject induced by M-CSF/RANKL. (B) Calcium signals in response to M-CSF/RANKL in Fura-2-loaded BMDMs from patients with the mutations STIM1$^{p.E136X}$, STIM1$^{p.r429c}$ and STIM1$^{p.r304w}$, as well as the healthy subject. (C) The proportion of Cd11b$^+$ and TRAP$^+$ cells detected by flow cytometry prior to and after treatment of STIM1$^{wt}$ or STIM1$^{mut}$ BMDMs with M-CSF/RANKL. (D) Cell proliferation of BMDMs at different time-points under M-CSF/RANKL treatment. (E and F) Intensity of (E) the CSFE fluorescence probe and (F) ki67 expression in BMDMs treated with M-CSF/RANKL. (G and H) Expression levels of (G) cathepsin K and (H) MMP9 following induction with RANKL/M-CSF. Values are expressed as the mean ± standard deviation (n=6). $^{**}$P<0.01 and $^{***}$P<0.001 vs. WT BMDMs or untreated BMDMs. BMDMs, bone marrow-derived mononuclear macrophages; STIM1, stromal interaction molecule 1; wt, wild-type; mut, mutant; MMP9, matrix metallopeptidase 9; TRAP, tartrate-resistant acid phosphatase; RANKL, receptor activator of NF-κB ligand; M-CSF, macrophage colony-stimulating factor; CSFE, carboxyfluorescein succinimidyl ester.

formation of osteoclasts is the result of the interaction between M-CSF and RANKL (1). Under the combined induction by RANKL/M-CSF, STIM1$^{wt}$ BMDMs (Cd11b$^{+}$) differentiated into osteoclasts (TRAP$^{+}$) and fused, whereas the STIM1$^{p.R429C}$ and STIM1$^{p.E136X}$ BMDMs exhibited significant reductions in RANKL/M-CSF-induced osteoclast differentiation, and the STIM1$^{R304W}$ BMDMs exhibited a significant increase in osteoclastogenesis (Fig. 2C). Similarity, the cell proliferation activity of the normal BMDMs increased in a time-dependent manner, whereas the STIM1$^{p.R429C}$ and STIM1$^{p.E136X}$ BMDMs exhibited a significant decrease and STIM1$^{p.R304W}$ BMDMs exhibited a significant increase in proliferation in response to RANKL/M-CSF treatment (Fig. 2D). CSFE is a nuclear fluorescent dye that indirectly represents the number of cell divisions. Ki67 is a cell cycle entry marker molecule that is expressed on all cells in the cell cycle except for those in G0 phase and indicates the degree of cell proliferation. The cell division ability and the number of cells entering the cell cycle were significantly higher in STIM1$^{wt}$ BMDMs compared with that in STIM1$^{p.R429C}$ and STIM1$^{p.E136X}$ BMDMs, and significantly lower compared with that in STIM1$^{p.R304W}$ BMDMs (Fig. 2E and F), under the combined induction of RANKL/M-CSF. Cathepsin K and MMP9 process a variety of biologically active molecules, participate in bone resorption of osteoclasts and indirectly reflect the bone resorption ability of osteoclasts (28,29). Cathepsin K and MMP9 process a variety of biologically active molecules, participate in bone resorption of osteoclasts and indirectly reflect the osteoclast ability of osteoclasts (30). Following stimulation by RANKL/M-CSF, the upregulation of Cathepsin K and MMP9 expression in STIM1$^{p.R304W}$ cells was more pronounced compared with that in the WT cells than STIM1$^{p.R429C}$ and STIM1$^{p.E136X}$ cells. (Fig. 2G and H). These results indicate that STIM1 is involved in RANKL/M-CSF-induced osteoclast proliferation, differentiation and bone resorption.

*STIM1 defects lead to abnormal osteoclastogenesis signalling in BMDMs*. Calcineurin is a target protein of intracellular $Ca^{2+}$ that enters by SOCE and exerts a wide range of physiological activities (31). RANKL/M-CSF induced a rapid increase in calcineurin activity in normal BMDMs, a comparatively greater increase in STIM1$^{p.R304W}$ BMDMs, a weaker increase in STIM1$^{p.R429C}$ and no response in STIM1$^{p.E136X}$ BMDMs (Fig. 3A). In the BMDMs from all subjects, calcineurin activity was inhibited by CsA (Fig. 3A), an immunosuppressant that targets the $Ca^{2+}$- and calmodulin-regulated phosphatase calcineurin and inhibits the activation of the Akt/mTOR signaling pathway (29). The Akt/mTOR pathway is essential for osteoclast development. Next, the effect of SOCE on RANKL/M-CSF-induced Akt/mTOR activity was explored. Due to the limited amount of precious cell samples, flow cytometry was used to detect the phosphorylation levels of intracellular protein kinases. The mTOR$^{S2448}$, Akt$^{S473}$ and Akt$^{T308}$ phosphorylation levels were significantly increased in the STIM1$^{wt}$ BMDMs following induction by RANKL/M-CSF (Fig. 3B-D). The Akt/mTOR activation levels were significantly higher in the STIM1$^{p.R304W}$ BMDMs and lower in the STIM1$^{p.R429C}$ BMDMs than those in the STIM1$^{wt}$ BMDMs, while the Akt/mTOR signal of STIM1$^{p.E136X}$ BMDMs did not respond to RANKL/M-CSF-induced activation (Fig. 3B-D). The phosphorylation level of p70 S6k, which is a substrate of mTOR, was significantly increased by RANKL induction. RANKL/M-CSF-induced activation of p70 S6k in STIM1$^{mut}$ BMDMs was consistent with the activation of Akt/mTOR signaling (Fig. 3E). Transcription factor NFATC2 is highly phosphorylated in resting cells, while dephosphorylation occurs with intracellular calcium-dependent calcineurin activation, followed by translocation to the nucleus (32). RANKL/M-CSF may induce dephosphorylation of STIM1$^{wt}$ BMDMs at NFATC2$^{Ser172}$, and the p-NFATC2 levels were significantly downregulated in the STIM1$^{p.R304W}$ and upregulated in the STIM1$^{p.R429C}$ BMDMs compared with those in the STIM1$^{wt}$ BMDMs, while the level of NFATC2 phosphorylation in STIM1$^{p.E136X}$ BMDMs was not altered following treatment with RANKL/M-CSF (Fig. 3F and G). To verify the effect of calcineurin/Akt/mTOR/NFATC2 signalling on RANKL/M-CSF-induced proliferation, the STIM1$^{wt}$ BMDMs were treated with the calcineurin inhibitor CsA, the mTOR inhibitor Rap and NFATC2-interfering RNA. The interference efficiency of NFATC2 siRNA is provided in Supplementary Fig. S1A-C. The results indicated that CsA, Rap and NFATC2 siRNA inhibited cell division and cell cycle entry, and reduced the expression of Ki67, cathepsin K and MMP9 (Fig. 3H). Similarly, CsA, Rap and NFATC2 siRNA inhibited the RANKL/M-CSF-induced proliferative activity and osteoclastogenesis (Fig. 3I and J). These results indicate that the calcineurin/Akt/mTOR/NFATC2 pathway is involved in SOCE-controlled cell proliferation, differentiation and osteoclastogenesis.

*Lentiviral transfection of STIM1 is not always able to restore disorders in osteoclastogenesis caused by its defects in vitro*. Lentiviral overexpression of plasmid expressing wild type STIM1 (ca.STIM1) was performed in an attempt to restore the RANKL/M-CSF-induced disorders of osteoclastogenesis caused by of STIM1 mutation (Fig. 4A, Supplementary Fig. S1C-D and F). Transfection of STIM1$^{wt}$ into BMDMs with caSTIM1 did not affect the amplitude and threshold of the calcium influx. This is because the upper limit of the calcium influx peak depends on the concentration of calcium stores in the ER and not the level of STIM1 expression (27). Transfection of ca.STIM1 restored calcium influx in STIM1$^{p.R429C}$ and STIM1$^{p.E136X}$ BMDMs in response to RANKL/M-CSF, but was not able to reverse the constitutive activation of SOCE in STIM1$^{p.R304W}$ BMDMs (Fig. 4B). This was most probably due to the residual constitutively active STIM1$^{p.R304W}$ protein. Regarding cell viability, caSTIM1 did not affect the proliferative activity of wild-type cells but restored the RANLK/M-CSF-induced proliferative disorder caused by the STIM1$^{p.R429C}$ and STIM1$^{p.E136X}$ mutations; however, caSTIM1 did not restore the proliferative disorder caused by the STIM1$^{p.R304W}$ mutation (Fig. 4C). In terms of cell differentiation, caSTIM1 did not affect STIM1$^{p.R304W}$ BMDMs but restored the impaired capacity of the STIM1$^{p.R429C}$ and STIM1$^{p.E136X}$ mutant cells to differentiate upon induction by RANLK/M-CSF (Fig. 4D). Although lentiviral transfection of caSTIM1 failed to restore the osteoclastogenesis capacity of STIM1$^{p.R304W}$ cells, inhibitors of calcineurin/Akt/mTOR signaling inhibited excessive differentiation and proliferation induced by RANLK/M-CSF *in vitro* (Fig. 4E and F). In addition, NFATC2 siRNA inhibited excessive differentiation and proliferation of STIM1$^{p.R304W}$

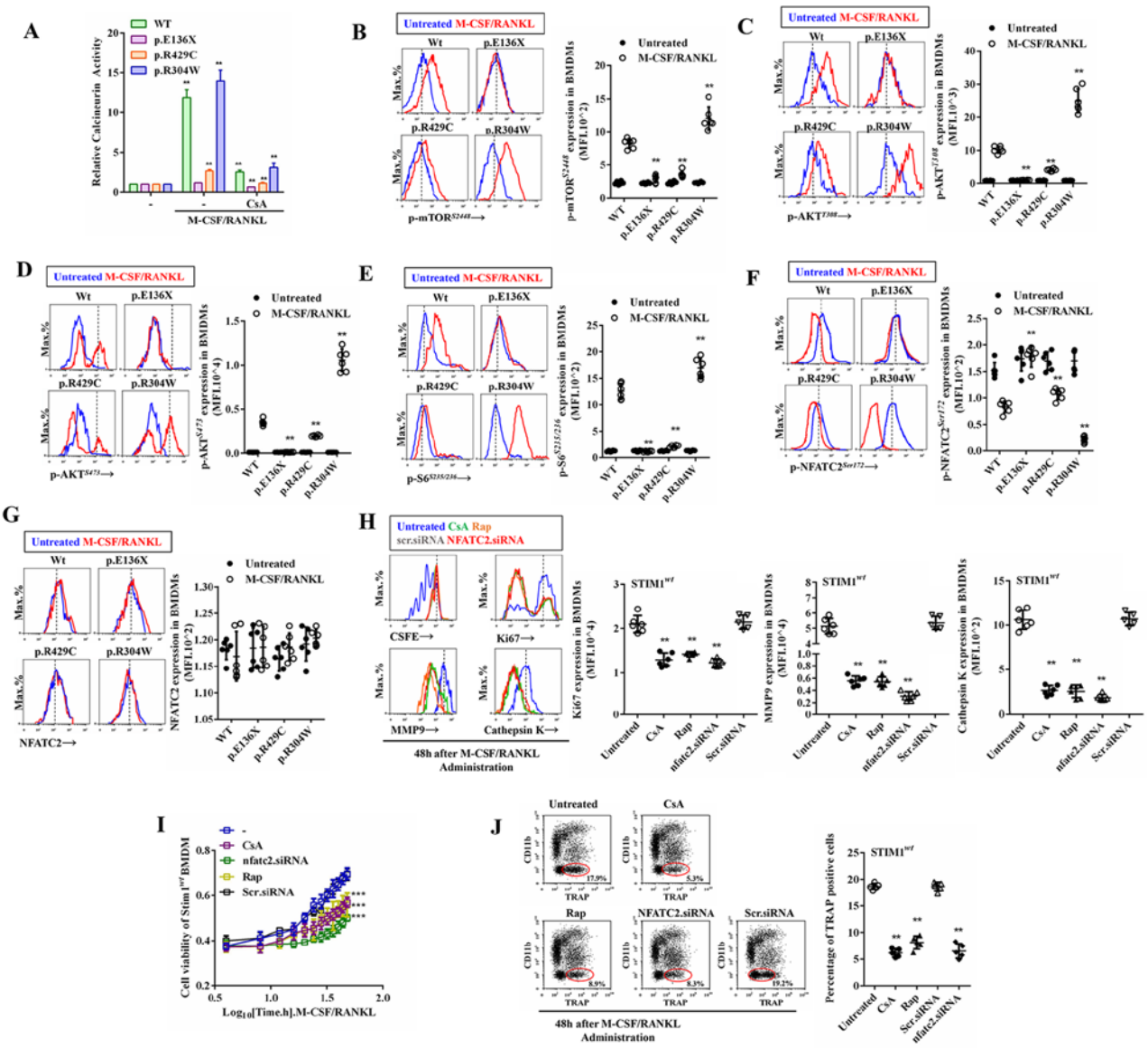


Figure 3. Calcineurin/Akt/mTOR/NFATC2 signalling controlled by store-operated $Ca^{2+}$ entry. (A) M-CSF/RANKL-induced calcineurin activity in BMDMs in the presence or absence of CsA. (B-G) Phosphorylation levels of (B) mTOR$^{S2448}$, (C) AktT$^{308}$, (D) Akt$^{S473}$, (E) p70$^{S6S235/236}$ and dephosphorylation levels of (F) NFATC2 and (G) total NFATC2 were detected by flow cytometry prior to and after treatment of STIM1$^{wt}$ or STIM1$^{mut}$ BMDMs with M-CSF/RANKL. (H) The CSFE fluorescence intensity, as well as the expression of ki67, cathepsin K and MMP9 in STIM1$^{wt}$ or STIM1$^{mut}$ BMDMs were detected prior to and after treatment with M-CSF/RANKL in the presence or absence of 7 nM CsA, 0.1 nM Rap or NFATC2 siRNA. (I) Proliferation and (J) differentiation of STIM1$^{wt}$ or STIM1$^{mut}$ BMDMs detected prior to and after treatment with M-CSF/RANKL in the presence or absence of 7 nM CsA, 0.1 nM Rap or NFATC2 siRNA. Values are expressed as the mean ± standard deviation (n=6). $^{**}$P<0.01 and $^{***}$P<0.001 vs. Untreated BMDMs. BMDMs, bone marrow-derived mononuclear macrophages; CSFE, carboxyfluorescein succinimidyl ester; STIM1, stromal interaction molecule 1; wt, wild-type; mut, mutant; MMP, matrix metallopeptidase; TRAP, tartrate-resistant acid phosphatase; RANKL, receptor activator of NF-κB ligand; M-CSF, macrophage colony-stimulating factor; siRNA, small interfering RNA; CsA, cyclosporin A; Rap, rapamycin; p-Akt, phosphorylated Akt.

BMDMs induced by RANLK/M-CSF (Fig. 4E and F). These results confirm the important role of SOCE in osteoclastogenesis and suggest the possibility of gene therapy for the treatment of congenital bone diseases.

## Discussion

$Ca^{2+}$ mediates a variety of cellular physiological functions by transmitting intracellular signals. Activation of membrane-receptor-coupled phospholipase Cγ produces inositol-1,4,5-trisphosphate, which binds to receptors on the ER membrane and stimulates $Ca^{2+}$ excretion into the ER, which triggers a wide range of physiological effects. After calcium storage in the ER is depleted, the cells activate ion channels to replenish intracellular and ER calcium; this process is called SOCE (33,34). ORAI and STIM are the two most important components of the SOCE process. STIM on the ER membrane pulls the ER membrane to the plasma membrane after $Ca^{2+}$ storage failure (35); the $Ca^{2+}$ release-activated $Ca^{2+}$ channel (CRAC) is formed by binding of STIM to the transmembrane channel protein ORAI on the membrane, and the opening of CRAC leads to SOCE (36-38). Therefore, SOCE is a calcium influx mode activated by the status of the ER calcium ion concentration. $Ca^{2+}$ entry into the intracellular phase through

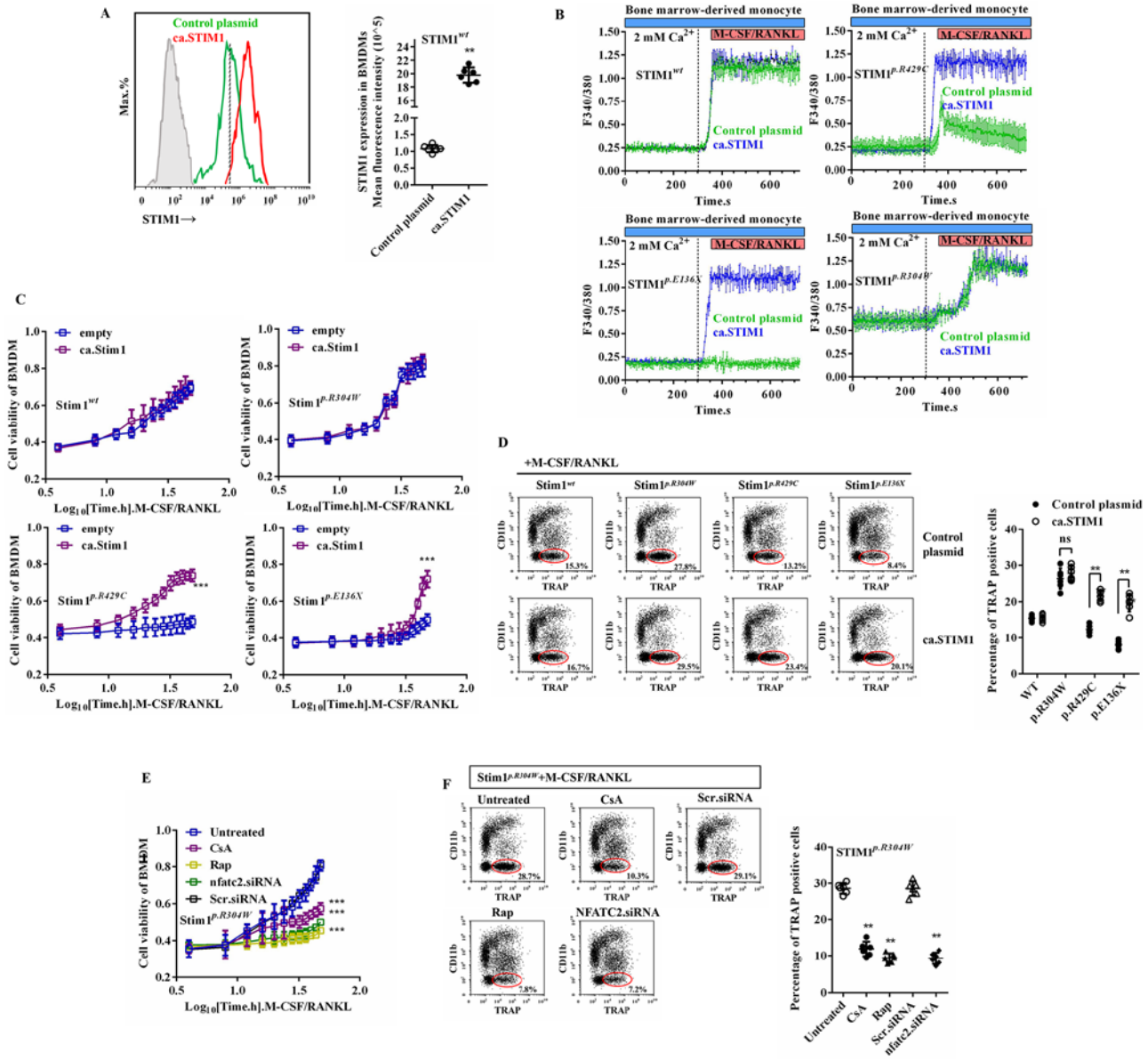


Figure 4. STIM1 overexpression restores store-operated $Ca^{2+}$ entry. (A) Reverse transcription lentiviral transfection efficiency of ca.STIM1 expression vector in the BMDMs. (B) $Ca^{2+}$ influx responses in Fura-2-loaded $STIM1^{wt}$ and $STIM1^{mut}$ BMDMs induced by M-CSF/RANKL following transfection with an empty plasmid or ca.STIM1, as measured using the 340/380 nm ratio. (C) Proliferation and (D) differentiation of the $STIM1^{wt}$ and $STIM1^{mut}$ BMDMs induced by M-CSF/RANKL following transfection with an empty plasmid or ca.STIM1. (E) Proliferation and (F) differentiation of the STIM1p.R304W BMDMs induced by M-CSF/RANKL following treatment with CsA, Rap and transfection with NFATC2 siRNA. Values are expressed as the mean ± standard deviation (n=6). $^{**}P<0.01$ and $^{***}P<0.001$ vs. Control plasmid or Untreated BMDMs; ns, no significance. BMDMs, bone marrow-derived mononuclear macrophages; STIM1, stromal interaction molecule 1; wt, wild-type; mut, mutant; MMP, matrix metallopeptidase; TRAP, tartrate-resistant acid phosphatase; RANKL, receptor activator of NF-κB ligand; M-CSF, macrophage colony-stimulating factor; siRNA, small interfering RNA; CsA, cyclosporin A; Rap, rapamycin.

SOCE may last from several minutes to several hours and drives a wide range of cellular functions, including secretion, gene transcription, cell contraction and phagocytosis (39). The disease caused by impaired SOCE function is called CRAC channel disease (40).

STIM1 is a dimeric transmembrane protein of the ER and the gene encoding STIM1 has 12 exons. A single insertion of an adenine nucleotide mutation at 380-381 leads to early termination of translation, resulting in the p.E136X nonsense mutant protein, which is characterized by protein truncation (26). Substitution mutations at positions 910 and 1,285 produce the p.R304W (27) and p.R429C (26) missense protein mutations, the former of which is associated with normal STIM1 expression, while the latter affects STIM1 expression. Due to loss of STIM1 expression or conformational changes, the normal function of SOCE of BMDMs was disrupted, including the abolition of SOCE caused by the p.E136X and p.R429C mutations and the sustained activation of SOCE associated with the p.R304W mutation. RANKL/M-CSF may induce stable and continuous calcium influx in BMDMs of healthy subjects. By contrast, $STIM1^{p.R429C}$ BMDMs only had a small amount of transient calcium influx, while $STIM1^{p.E136X}$ BMDMs did not respond to induction of calcium influx by RANKL/M-CSF. The basal intracellular concentration of quiescent $STIM1^{p.R304W}$ BMDMs was significantly increased and peaked rapidly under induction with RANKL/M-CSF. In

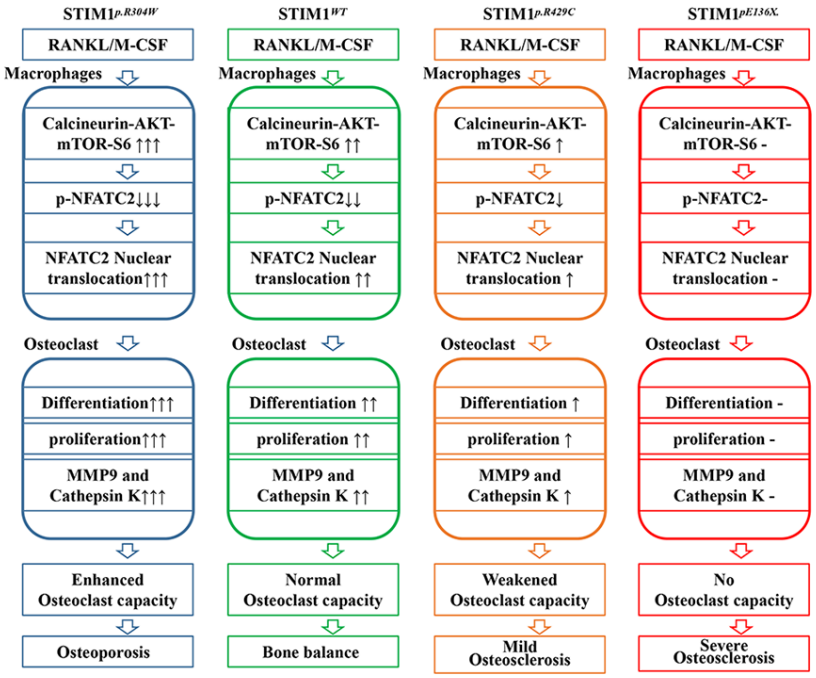


Figure 5. Schematic illustrating different ways of STIM1 mutations to affect the store-operated $Ca^{2+}$ entry controls and calcineurin/Akt/mTOR/NFATC2-mediated osteoclastogenesis induced by RANKL/M-CSF. RANKL, receptor activator of NF-κB ligand; M-CSF, macrophage colony-stimulating factor; STIM1, stromal interaction molecule 1; MMP, matrix metallopeptidase.

spite of having the same STIM1 mutation, these three patients had opposite bone metabolic diseases, including osteosclerosis in those with the p.E136X and p.R429C mutations and bone loss in the patient with the p.R304W mutation. These studies observed the possible effects of STIM1 mutations on abnormal bone metabolism in CID patients.

M-CSF promotes the proliferation and survival of osteoclast precursor cells through its receptor M-CSFR via phosphoinositide 3-kinase (PI3K)/Akt signalling (41,42). The RANKL-mediated NF-κB, MAPK and PI3K/Akt signalling pathways are required to activate NFATC2 in osteoclasts (43). Therefore, RANKL/M-CSF synergistically promotes osteoclast survival and differentiation. The differentiation of BMDMs from healthy subjects into $TRAP^+$ cells increased by about 17% under induction by RANKL/M-CSF, the p.R429C mutation significantly reduced $TRAP^+$ cell production, whereas the p.E136X mutation was associated with only a minor response to RANKL/M-CSF induction. By contrast, p.R304W mutation led to production of a large amount of $TRAP^+$ cells under the induction of RANKL/M-CSF. Following RANKL/M-CSF induction, the cell viability, cell cycle entry and cell division abilities of the $STIM1^{mut}$ BMDMs were different from those of the healthy control cells. The $STIM1^{p.R429C}$ BMDMs had a reduced proliferate tendency, while that of the $STIM1^{p.R304W}$ BMDMs was enhanced, and the $STIM1^{p.E136X}$ BMDMs did not proliferate at all. Cathepsin K and MMP9 are markers of osteoclastogenesis and functional enzymes that exert osteolysis. RANKL/M-CSF-induced cathepsin K and MMP9 expression were different between the $STIM1^{mut}$ and $STIM1^{wt}$ BMDMs, including reduced expression in $STIM1^{p.R429C}$ BMDMs, increased expression in $STIM1^{p.R304W}$ BMDMs and unaffected in $STIM1^{p.E136X}$ BMDMs. These results suggest that the absence of functional STIM1 affects survival, osteoclastogenesis and function of BMDMs.

mTOR is an atypical serine/threonine kinase that exists in two different mTOR complexes. mTOR complex 1, which is composed of mTOR, raptor, GβL and DEPTOR, is inhibited by rapamycin (44). Studies of RANKL-induced osteoclast differentiation have clearly confirmed that these cells undergo regulation of calcineurin activity and that negative feedback regulates NFATC2-mediated osteoclastogenesis and bone resorption (28). In the present study, the calcineurin activity of the $STIM1^{mut}$ BMDMs was different from that of the $STIM1^{wt}$ BMDMs in presence of RANKL/M-CSF: That of $STIM1^{p.R429C}$ BMDMs was weakened, that of $STIM1^{p.R304W}$ BMDMs was enhanced and that of $STIM1^{p.E136X}$ was not affected. Similarly, the RANKL/M-CSF-induced phosphorylation levels of $mTOR^{S2448}$ and the mTOR substrate p70 $S6^{S235/236}$ were significantly higher in the $STIM1^{p.R304W}$ BMDMs than those in the $STIM1^{wt}$ BMDMs, and the phosphorylation levels of $Akt^{S473}$ and $Akt^{T308}$ were also significantly higher than those in the $STIM1^{p.R304W}$ BMDMs. Attenuated Akt/mTOR-S6 signaling was observed in $STIM1^{p.R429C}$ BMDMs, while no response activation of these signals was observed in $STIM1^{p.E136X}$ BMDMs. in addition, the RANKL/M-CSF-induced dephosphorylation levels of NFATC2 were significantly higher in the $STIM1^{p.R304W}$ BMDMs and lower in the $STIM1^{p.R429C}$ BMDMs than in the $STIM1^{wt}$ BMDMs, and no response dephosphorylation of NFATC2 was observed in $STIM1^{p.E136X}$ BMDMs. Calcineurin inhibitor CsA and mTOR inhibitors rapamycin and NFATC2 siRNA inhibited RANKL/M-CSF-induced osteoclastogenesis of BMDMs. This result directly indicates that NFATC2 is involved in osteoclastogenesis disorders caused by SOCE deficiency.

Finally, STIM1-deficient BMDMs were transfected with STIM1 overexpression plasmids. SOCE-dependent calcium influx does not depend on the expression level of STIM1 or ORAI1; rather, it depends on whether the ER $Ca^{2+}$ is 'storage-depleted'. M-CSF/RANKL stimulates intracellular signal activation and consumes ER $Ca^{2+}$. When the $Ca^{2+}$ stored in the ER is consumed, the $Ca^{2+}$ concentration sensor STIM1 on the ER and the $Ca^{2+}$ channel STIM1 on the cytoplasmic membrane are physically combined, thereby causing $Ca^{2+}$ influx. Since STIM1 in patients with p.E136X and p.R429C mutations was completely inactivated, SOCE-$Ca^{2+}$ influx did not occur in response to M-CSF/RANKL-induced activation. Of note, transfection of caSTIM1 for overexpression was able to restore normal SOCE in these cells. At the same time, the SOCE channel in $STIM1^{p.R304W}$ BMDMs is continuously activated, so the basic intracellular $Ca^{2+}$ concentration is higher than that of normal cells. However, as the STIM1 still carried a conformational mutation, caSTIM1 cannot restore normal SOCE in $STIM1^{p.R304W}$ BMDMs. In addition, the RANKL/M-CSF-induced persistent stable calcium influx, and the proliferation and differentiation into osteoclasts that were reduced due to p.E136X and p.R429C mutation-associated STIM1 deficiency were restored *in vitro*. In turn, CsA, Rap and NFATC2 siRNA were able to recover the RANKL/M-CSF-induced proliferation and differentiation that were reduced by p.E136X and p.R429C mutation-associated STIM1 deficiency. These results suggest the potential ability of gene therapy to treat congenital bone loss or osteopetrosis.

In conclusion, the present study confirmed that SOCE was involved in the survival, differentiation and function of osteoclasts. As presented in Fig. 5, different mutations in STIM1 affect the function of SOCE in different ways, which leads to abnormalities of calcineurin/Akt/mTOR/S6 phosphorylation and NFATC2 dephosphorylation, and results in aberrant differentiation, proliferation and osteoclast differentiation of BMDMs, which leads to different types of bone metabolic disorder.

**Acknowledgements**

Not applicable.

**Funding**

The present study was funded by the Key Research Project of Wannan Medical College (grant no. WK2017Z07) and the National Natural Science Foundation of China (grant no. 81800082).

**Availability of data and materials**

The datasets used and/or analyzed during the present study are available from the corresponding author on reasonable request.

**Authors' contributions**

YJH and QL were a major contributor in acquisition of data, ZYF was a major contributor in analysis and interpretation of data, LRZ was a major contributor in conception, design and writing the manuscript. All authors read and approved the final manuscript.

**Ethical approval and consent to participate**

The experiments involving human subjects were based on the Declaration of Helsinki and the European Declaration of Human Rights. The study was approved by the Ethical Review Committee of Yanjishan Hospital of Wannan Medical College (Wuhu, China; no. 201627).

**Patient consent for publication**

Informed consent was obtained from the parents of the patients and the healthy donor.

**Competing interests**

The authors declare that they have no competing interests.

**References**

1. Boyle WJ, Simonet WS and Lacey DL: Osteoclast differentiation and activation. Nature 423: 337-342, 2003.
2. Harada S and Rodan GA: Control of osteoblast function and regulation of bone mass. Nature 423: 349-355, 2003.
3. Zaidi M: Skeletal remodeling in health and disease. Nat Med 13: 791-801, 2007.
4. Kobayashi E and Setsu N: Osteosclerosis induced by denosumab. Lancet 7: 539, 2015.
5. Luo J, Yang Z, Ma Y, Yue Z, Lin H, Qu G, Huang J, Dai W, Li C, Zheng C, *et al*: LGR4 is a receptor for RANKL and negatively regulates osteoclast differentiation and bone resorption. Nat Med 22: 539-546, 2016.
6. Fu J, Li S, Feng R, Ma H, Sabeh F, Roodman GD, Wang J, Robinson S, Guo XE, Lund T, *et al*: Multiple myeloma-derived MMP-13 mediates osteoclast fusogenesis and osteolytic disease. J Clin Invest 126: 1759-1772, 2016.
7. Okamoto K, Nakashima T, Shinohara M, Negishi-Koga T, Komatsu N, Terashima A, Sawa S, Nitta T and Takayanagi H: Osteoimmunology: The conceptual framework unifying the immune and skeletal systems. Physiol Rev 97: 1295-1349, 2017.
8. Chen X, Zhi X, Cao L, Weng W, Pan P, Hu H, Liu C, Zhao Q, Zhou Q, Cui J and Su J: Matrine derivate MASM uncovers a novel function for ribosomal protein S5 in osteoclastogenesis and postmenopausal osteoporosis. Cell Death Dis 8: e3037, 2017.
9. Suematsu A, Nakashima T, Takemoto-Kimura S, Aoki K, Morishita Y, Asahara H, Ohya K, Yamaguchi A, Takai T, Kodama T, *et al*: Regulation of osteoclast differentiation and function by the CaMK-CREB pathway. Nat Med 17: 1410-1416, 2006.
10. Ortuño MJ, Robinson ST, Subramanyam P, Paone R, Huang YY, Guo XE, Colecraft HM, Mann JJ and Ducy P: Serotonin-reuptake inhibitors act centrally to cause bone loss in mice by counteracting a local anti-resorptive effect. Nat Med 22: 1170-1179, 2016.
11. Xu S, Zhang Y, Wang J, Li K, Tan K, Liang K, Shen J, Cai D, Jin D, Li M, *et al*: TSC1 regulates osteoclast podosome organization and bone resorption through mTORC1 and Rac1/Cdc42. Cell Death Differ 25: 1549-1566, 2018.
12. Hoefle G, Holzmueller H and Drexel H: Alendronate versus calcitriol for prevention of bone loss after cardiac transplantation. N Engl J Med 350: 2306-2308, 2004.
13. Janssen NM and Genta MS: The effects of immunosuppressive and anti-inflammatory medications on fertility, pregnancy, and lactation. Arch Intern Med 160: 610-619, 2000.
14. Huynh H, Wei W and Wan Y: mTOR inhibition subdues milk disorder caused by maternal VLDLR loss. Cell Rep 19: 2014-2025, 2017.
15. Zhou C, You Y, Shen W, Zhu YZ, Peng J, Feng HT, Wang Y, Li D, Shao WW, Li CX, *et al*: Deficiency of sorting nexin 10 prevents bone erosion in collagen-induced mouse arthritis through promoting NFATc1 degradation. Ann Rheum Dis 75: 1211-1218, 2016.
16. Takayanagi H, Kim S, Koga T, Nishina H, Isshiki M, Yoshida H, Saiura A, Isobe M, Yokochi T, Inoue J, *et al*: Induction and activation of the transcription factor NFATc1 (NFAT2) integrate RANKL signaling in terminal differentiation of osteoclasts. Dev Cell 3: 889-901, 2002.

17. Kim H, Kim T, Jeong BC, Cho IT, Han D, Takegahara N, Negishi-Koga T, Takayanagi H, Lee JH, Sul JY, *et al*: Tmem64 modulates calcium signaling during RANKL-mediated osteoclast differentiation. Cell Metab 17: 249-260, 2013.
18. Masuyama R, Vriens J, Voets T, Karashima Y, Owsianik G, Vennekens R, Lieben L, Torrekens S, Moermans K, Vanden Bosch A, *et al*: TRPV4-mediated calcium influx regulates terminal differentiation of osteoclasts. Cell Metab 8: 257-265, 2008.
19. Hwang SY and Putney JW: Orai1-mediated calcium entry plays a critical role in osteoclast differentiation and function by regulating activation of the transcription factor NFATc1. FASEB J 26: 1484-1492, 2012.
20. Crabtree NJ, Shaw NJ, Bishop NJ, Adams JE, Mughal MZ, Arundel P, Fewtrell MS, Ahmed SF, Treadgold LA, Högler W, *et al*: Amalgamated reference data for size-adjusted bone densitometry measurements in 3598 children and young adults-the ALPHABET study. J Bone Miner Res 32: 172-180, 2017.
21. Guo B, Xu Y, Gong J, Tang Y and Xu H: Age trends of bone mineral density and percentile curves in healthy Chinese children and adolescents. J Bone Miner Metab 31: 304-314, 2013.
22. Notredame C, Higgins DG and Heringa J: T-Coffee: A novel method for fast and accurate multiple sequence alignment. J Mol Biol 302: 205-217, 2000.
23. Huang Z, Ruan HB, Xian L, Chen W, Jiang S, Song A, Wang Q, Shi P, Gu X and Gao X: The stem cell factor/Kit signalling pathway regulates mitochondrial function and energy expenditure. Nat Commun 5: 4282, 2014.
24. Misceo D, Holmgren A, Louch WE, Holme PA, Mizobuchi M, Morales RJ, De Paula AM, Stray-Pedersen A, Lyle R, Dalhus B, *et al*: A dominant STIM1 mutation causes Stormorken syndrome. Hum Mutat 35: 556-564, 2014.
25. Picard C, Mccarl CA, Papolos A, Khalil S, Lüthy K, Hivroz C, LeDeist F, Rieux-Laucat F, Rechavi G, Rao A, *et al*: STIM1 mutation associated with a syndrome of immunodeficiency and autoimmunity. N Engl J Med 360: 1971-1980, 2009.
26. Maus M, Jairaman A, Stathopulos PB, Muik M, Fahrner M, Weidinger C, Benson M, Fuchs S, Ehl S, Romanin C, *et al*: Missense mutation in immunodeficient patients shows the multifunctional roles of coiled-coil domain 3 (CC3) in STIM1 activation. Proc Natl Acad Sci USA 112: 6206-6211, 2015.
27. Morin G, Bruechle NO, Singh AR, Knopp C, Jedraszak G, Elbracht M, Brémond-Gignac D, Hartmann K, Sevestre H, Deutz P, *et al*: Gain-of-function mutation in STIM1 (P.R304W) is associated with Stormorken syndrome. Hum Mutat 35: 1221-1232, 2015.
28. Vaeth M, Maus M, Klein-Hessling S, Freinkman E, Yang J, Eckstein M, Cameron S, Turvey SE, Serfling E, Berberich-Siebelt F, *et al*: Store-operated $Ca^{2+}$ entry controls clonal expansion of T cells through metabolic reprogramming. Immunity 47: 664-679.e6, 2017.
29. Li CH, Yang ZF, Li ZX, Ma Y, Zhang L, Zheng C, Qiu W, Wu X, Wang X, Li H, *et al*: Maslinic acid suppresses osteoclastogenesis and prevents ovariectomy-induced bone loss by regulating RANKL-mediated NF-κB and MAPK signaling pathways. J Bone Miner Res 26: 644-656, 2011.
30. Ohta K, Naruse T, Ishida Y, Shigeishi H, Nakagawa T, Fukui A, Nishi H, Sasaki K, Ogawa I and Takechi M: TNF-α-induced IL-6 and MMP-9 expression in immortalized ameloblastoma cell line established by hTERT. Oral Dis 23: 199-209, 2017.
31. Huynh H and Wan Y: mTORC1 impedes osteoclast differentiation via calcineurin and NFATc1. Commun Biol 1: 29, 2018.
32. Hogan PG, Chen L, Nardone J and Rao A: Transcriptional regulation by calcium, calcineurin, and NFAT. Genes Dev 15: 2205-2232, 2003.
33. Cahalan MD: STIMulating store-operated Ca(2+) entry. Nat Cell Biol 11: 669-677, 2009.
34. Lewis RS: The molecular choreography of a store-operated calcium channel. Nature 446: 284-287, 2007.
35. Roos J, DiGregorio PJ, Yeromin AV, Ohlsen K, Lioudyno M, Zhang S, Safrina O, Kozak JA, Wagner SL, Cahalan MD, *et al*: STIM1, an essential and conserved component of store-operated Ca2+ channel function. J Cell Biol 169: 435-445, 2005.
36. Feske S, Gwack Y, Prakriya M, Srikanth S, Puppel SH, Tanasa B, Hogan PG, Lewis RS, Daly M and Rao A: A mutation in Orai1 causes immune deficiency by abrogating CRAC channel function. Nature 441: 179-185, 2006.
37. Vig M, Peinelt C, Beck A, Koomoa DL, Rabah D, Koblan-Huberson M, Kraft S, Turner H, Fleig A, Penner R and Kinet JP: CRACM1 is a plasma membrane protein essential for store-operated Ca2+ entry. Science 312: 1220-1223, 2006.
38. Zhang SL, Yeromin AV, Zhang XH, Yu Y, Safrina O, Penna A, Roos J, Stauderman KA and Cahalan MD: Genome-wide RNAi screen of Ca(2+) influx identifies genes that regulate Ca(2+) release-activated Ca(2+) channel activity. Proc Natl Acad Sci USA 103: 9357-9362, 2006.
39. Feske S, Skolnik EY and Prakriya M: Ion channels and transporters in lymphocyte function and immunity. Nat Rev Immunol 12: 532-547, 2012.
40. Parekh AB: Store-operated CRAC channels: Function in health and disease. Nat Rev Drug Discov 9: 399-410, 2010.
41. Wang L, Iorio C, Yan K, Yang H, Takeshita S, Kang S, Neel BG and Yang W: A ERK/RSK-mediated negative feedback loop regulates M-CSF-evoked PI3K/AKT activation in macrophages. FASEB J 32: 875-887, 2018.
42. Pacitto R, Gaeta I, Swanson JA and Yoshida S: CXCL12-induced macropinocytosis modulates two distinct pathways to activate mTORC1 in macrophages. J Leukoc Biol 101: 683-692, 2017.
43. Walsh MC and Choi Y: Biology of the RANKL-RANK-OPG system in immunity, bone, and beyond. Front Immunol 5: 511, 2014.
44. Dowling RJ, Topisirovic I, Fonseca BD and Sonenberg N: Dissecting the role of mTOR: Lessons from mTOR inhibitors. Biochim Biophys Acta 1804: 433-439, 2010.